Journal of Materials Chemistry C

ROYAL SOCIETY OF CHEMISTRY

PAPER

View Article Online
View Journal | View Issue

Cite this: *J. Mater. Chem. C*, 2023, **11**, 8293

On the factors affecting the response time of synaptic ion-gated transistors†

Ramin Karimi Azari, * Tian Lan and Clara Santato *

Received 14th January 2023,
Accepted 10th May 2023

DOI: 10.1039/d3tc00161j

rsc.li/materials-c

Ion-Gated Transistors (IGTs) feature the processing rate of the human brain for neuromorphic computing. Furthermore, they require low power for training and deployment of neural network algorithms. Neuromorphic computing requires both long-term and short-term potentiation, within the same device. The nature of the doping mechanism in IGTs affects their time-resolved properties, key for their use as neuromorphic devices. Depending on the permeability of the semiconducting channel to ions, IGTs undergo electrochemical (three-dimensional) or electrostatic (field-effect, two-dimensional) doping, which leads to a wide range of IGT response times. Here, we propose a methodology to control the response time of IGTs made up of films of poly(3-hexylthiophene (P3HT) as the semiconducting channel and the ionic liquid 1-ethyl-3-methylimidazolium bis(trifluoromethanesulfonyl)imide [EMIM][TFSI] as the gating medium. The methodology includes the effect of the pulse frequency of the applied gate-source voltage (V_{gs}), the number of applied V_{gs} pulses, and the V_{gs} pulse duration. It also considers the effect of the values of the applied V_{gs} and drain-source (V_{ds}) voltages. Last but not least, the methodology includes the effect of the V_{gs} sampling time. Our results contribute to the understanding of how to achieve plasticity in IGTs.

Published on 11 5 2023. Downloaded on 2024-07-16 5:10:48.

10th Anniversary Statement

In a battery, we find both electronic and ionic conduction. These two types of conduction also coexist in ion-gated transistors (IGTs), making use of ionic gating media (*e.g.* saline aqueous solutions and ionic liquids). IGTs are relevant for flexible and printable electronics, and bioelectronics. Furthermore, a three-terminal IGT closely resembles the biological synapse since the gate electrode acts as a neuron that applies the presynaptic spike and generates a postsynaptic current spike in the semiconducting channel, acting as a postsynaptic neuron. In this work, we propose a methodology that achieves synaptic plasticity in IGTs. We demonstrate that IGTs can be employed as neuromorphic devices integrating memory (long-term plasticity) and processing functions (short-term plasticity) in the same device, as a function of the electrical biasing conditions. We think that by reaching the convergence of electronic materials, ionic materials, low power electronics, device engineering, and neurosciences, our work can help to celebrate the 10th anniversary issue of the *Journal of Materials Chemistry C*.

Introduction

Ion-Gated Transistors (IGTs) make use of ionic compounds as the gating media. IGTs play a crucial role in the development of neuromorphic computing devices, due to their low operating voltages (sub-1 V), viable functionalization of the semiconducting channel for chemo and biosensing purposes, and possible fabrication into large device arrays.[1,2] Due to their combined electronic and ionic transport,[3–5] IGTs are relevant for future computation, bioelectronics, and electrochemical energy storage.[6–11]

Since the electrical double layer (EDL) at the interface between the semiconducting transistor channel and the ion gating medium is thin (3–4 nm), the specific capacitance observed in IGTs can be as high as 10 μF cm^{-2}, resulting in a large density of charge carriers (about 3 × 10^{15} cm^{-2}), at low V_{gs} biases.[12–14]

Several working mechanisms are possible for IGTs based on organic semiconducting channel materials, depending on the degree of permeability of the channel to ions. Ion-impermeable channels are electrostatically doped (as in conventional field-effect transistors, where the doping is *bidimensional*) whereas ion-permeable channels can be electrochemically doped (in this case the doping is three-dimensional).[15]

Certainly, IGTs can feature a combination of these two working mechanisms, where the weight of each contribution depends on the specific semiconductor and gating medium,

Engineering Physics, Polytechnique Montreal, 2500 Ch. Polytechnique, H3T 1J4, Montreal, QC, Canada

† Electronic supplementary information (ESI) available. See DOI: **https://doi.org/10.1039/d3tc00161j**

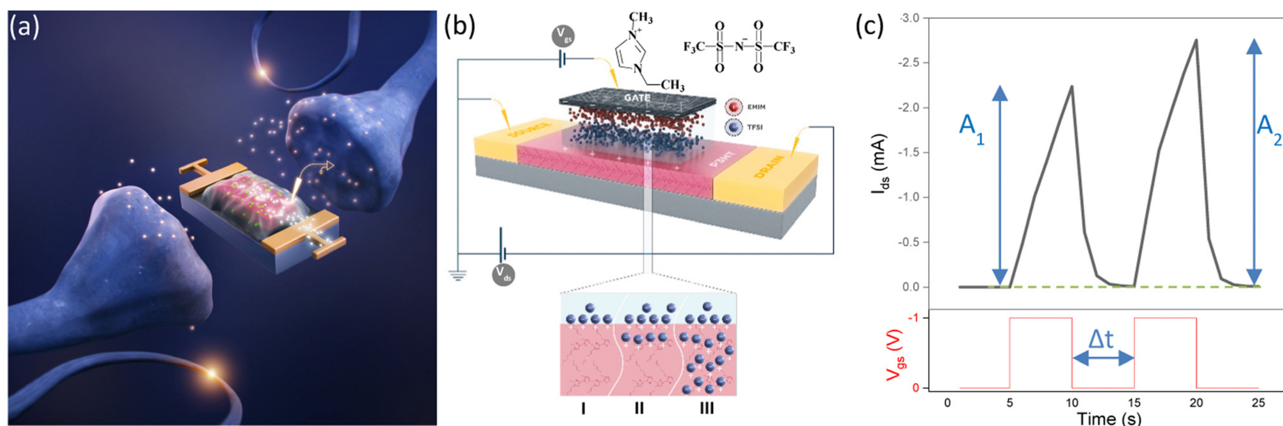

Fig. 1 (a) Bio-inspired synaptic IGT transistor. (b) Device scheme and possible doping regimes (I to III) upon application of a negative V_{gs} to a P3HT-based IGT; molecular structures of the ions constituting the ionic liquid employed as gating medium in this study. (c) A pair of successive V_{gs} inputs (−1 V) for 5 s with a pulse interval Δt = 5 s applied to an IGT. A_1 and A_2 are the amplitudes of the drain–source current (I_{ds}).

Published on 11 5 2023. Downloaded on 2024-07-16 5:10:48.

the quality of their interface, and the electrical biasing conditions. For instance, in organic single crystal channels poorly permeable to ions, upon application of a gate-source voltage (V_{gs}), ions accumulate at the ionic medium–organic semiconductor interface, bringing about electrostatic doping.[14,16–19]

The nature of the ionic medium (*e.g.*, solid, gel, or liquid) influences the movement of the ions in the gating media of IGTs, in turn affecting the transistor performance and response time.[10,20–24]

Room-temperature ionic liquids (ILs) are ideal gating media for IGTs since they feature a high conductivity (0.1–20 mS cm^{-1}), a wide range of viscosity (10–1000 mPa s), and minimal volatility.[25,26] Furthermore, their electrochemical stability window can be as high as 5 V.[16,27,28]

We can establish a correspondence between the working principle of IGTs and fundamental processes taking place in the brain (Fig. 1a). In the human brain, a neuronal network of around 10^{11} neurons is linked by approximately 10^{15} synapses. Synapses are a passageway for conveying action potentials from presynaptic to postsynaptic neurons. They carry out parallel information computing (processing and memorizing information) by adjusting the synaptic weight, *i.e.* the strength of a synaptic connection[29] (with the term synaptic strength referring to the amount of current generated in the postsynaptic neuron as a result of an action potential in the presynaptic neurons).

The rate of enhancement in the current amplitude after the second of two repetitive excitatory postsynaptic potentials (EPSPs) with an interval Δt is an index of the increase of the synaptic strength in a synaptic transistor, measured as paired pulse facilitation (PPF), defined as $(A_2-A_1)/A_1 \times 100$ (Fig. 1c).[30]

The three-terminal IGT closely resembles the biological synapse (Fig. 1a and b) since the gate electrode acts as a neuron that applies the presynaptic spike (V_{gs}) and generates a postsynaptic current (PSC) spike in the semiconducting channel (acting as a postsynaptic neuron) between source and drain electrodes (drain–source current, I_{ds}).

In an IGT artificial synapse, the synaptic plasticity can be described as the alteration of the synaptic weight and the IGT channel conductivity.[9] The synaptic weight is modulated independently *via* the gate terminal, in an IGT.[31] Short-term plasticity (STP) and long-term plasticity (LTP) are two categories of synaptic plasticity. A persistent modification of synaptic weight, LTP, supports memory and learning and lasts longer than a transient modification, STP. STP is necessary for data processing, encoding and filtering.[32,33]

An important aspect of synaptic plasticity modulation in IGTs is its response time, *e.g.*, the time it takes for the PSC of a transistor to reach a steady state after removal of the V_{gs} bias.

Response time can vary depending on the specific device structure, materials, and operating conditions.

We can consider two contributions to the I_{ds} decay in IGTs. The former is a fast current decay due to the removal of electrical double layers and/or ions located within a thin depth in the channel. The latter is a slow current decay related to the removal of the ions located deep in the channel and/or trapped.[10,24,34,35]

According to Bernards,[10] in IGTs, the response time of I_{ds} with respect to a change in V_{gs} can be fit by exponential functions. $I_{ds}(t)$ for the case of a square V_{gs} step follows a time dependence given by

$$I_{ds}(t) = I_{ss}(V_{gs}) + \Delta I_{ss}\left[1 - f\frac{\tau_e}{\tau_i}\right]e^{-\frac{t}{\tau_i}} \quad (1)$$

where $I_{ds}(t)$ is I_{ds} at time t, $I_{ss}(V_{gs})$ is the drain current at V_{gs}, ΔI_{ss} is the difference between the initial and final (steady state) drain currents, f is the weighting factor, τ_e is the electronic transit time along the channel, and τ_i is the time constant related to the $I_{ds}(t)$ decay rate, *i.e.* the transistor response time.

The majority of organic synaptic devices can only partially mimic synaptic plasticity, either LTP or STP, depending on the doping mechanism. One of the most significant challenges in IGTs is to transition plasticity from STP to LTP and *vice versa* in a single device and control the response time for various applications.[36–38] To tackle this challenge, aspects pertaining to the chemical nature and structure of the channel material

This journal is © The Royal Society of Chemistry 2023

Published on 11 5 2023. Downloaded on 2024-07-16 5:10:48.

and ionic medium, device structure and electrical bias input stimuli, should be all considered.[29]

In this study, we control the synaptic plasticity and response time of IGTs by controlling input V_{gs} and V_{ds} stimuli to modulate STP and LTP. We employed poly(3-hexylthiophene) (P3HT) as the organic transistor channel material, gated with the ionic liquid (1-ethyl-3-methylimidazolium bis(trifluoromethanesulfonyl)imide) ([EMIM][TFSI]) (Fig. 1b). We studied various aspects of bio-inspired synaptic transmission in [EMIM][TFSI]-gated P3HT transistors, such as spike frequency-dependent plasticity (SFDP) (defined as $(A_5-A_1)/A_1 \times 100$ for different frequencies of V_{gs} for a train of five pulses) and spike number-dependent plasticity (SNDP) (defined as $(A_n - A_1)/A_1 \times 100\%$ where $n > 1$ is the number of V_{gs} pulse). Furthermore, we investigated the influence of the sampling time of applied V_{gs} on the measured response time.

Results and discussion

Film morphology

AFM images show that the spin-coated P3TH films are continuous, with a root mean square (rms) roughness of *ca.* 3.77 ± 1.04 nm in a 10 μm × 10 μm-sized area (Fig S1a–c, ESI†). The XRD patterns of the P3HT films show a peak related to the lamellar structure located at $2\theta = 5.1°$ (Fig. S1d, ESI†).[39]

Transfer and output characteristics of [EMIM][TFSI]-gated P3HT transistors

The IGT transfer and output characteristics show a typical p-type behavior of transistors working in accumulation mode. We observed that the hysteresis decreases with the V_{gs} scan rate from 100 to 5 mV s^{-1} due to the increased time available to accommodate ion movement (Fig. 2a and Fig. S2a–c, ESI†). We deduced a threshold voltage of *ca.* −0.4 V, ON/OFF of *ca.* 10^2, mobility of 0.1 cm^2 V^{-1} s^{-1}, and charge carrier density of 3.0×10^{15} cm^{-2}, at 100 mV s^{-1} (values obtained at 50, 25, and 5 mV s^{-1} are reported in Table S1, ESI†).

Influence of the value of V_{gs} on the response time

We performed a typical I_{ds} transient response characterization (Fig. 2b and c) using a 200 ms-long square V_{gs} pulse with amplitudes −0.5 and −1 V, at V_{ds} = −0.2, −0.6, −0.8, and −1 V. Low amplitude V_{gs} (pre-synaptic spike) pulses are expected to induce the formation of electrical double layers and dope regions in P3HT close to the interface and/or amorphous. These regions can rapidly de-dope and PSC rapidly decays; this response is analogous to STP. We observed that the response time increased with the increase of V_{gs}. For instance, increasing V_{gs} from −0.5 V to −1 V (V_{ds} = −1 V) increases the response time from 7.31 to 9.33 ms, *i.e.* by 27%. Higher values of V_{gs} induce a deeper anion penetration in the film, possibly including crystalline

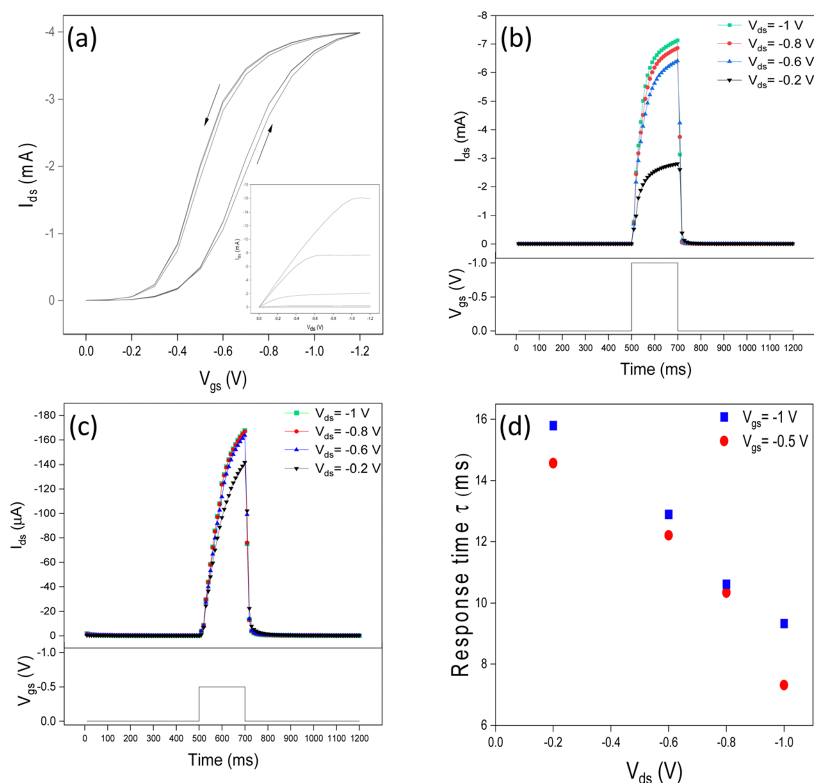

Fig. 2 Characteristics of [EMIM][TFSI]-gated P3HT transistors. (a) Transfer characteristics in the linear regime (V_{ds} = −0.2 V, (3 cycles)) at V_{gs} 100 mV s^{-1} scan rate (inset: output characteristic with V_{gs} = 0, −0.2, −0.4, −0.6, −0.8, −1 V and V_{ds} 100 mV s^{-1} scan rate). I_{ds} response to (b) V_{gs} = −1 V, (c) V_{gs} = −0.5 V, at different V_{ds}. The duration time of the V_{gs} bias is 200 ms. (d) Transient response of an [EMIM][TFSI]-gated P3HT transistor *versus* V_{ds} in different values of V_{gs} square step.

Published on 11 5 2023. Downloaded on 2024-07-16 5:10:48.

regions. This implies longer times for ion removal prior reaching the steady state, after the removal of V_{gs} (Fig. 2d).

Influence of the value of V_{ds} on the response time

We observed that the response time halves in a quasi-linear trend, in the region of V_{gs} included between −0.5 V and −1 V (Fig. 2d). According to Bernards' model (eqn (1)), the ratio τ_e/τ_i is determined by $\tau_e/\tau_i \sim dL^2/\mu V_{ds}^{-1}$ where d is the ionic gating medium thickness, L is the channel length and other symbols have been already introduced. In agreement with the model, the increase of V_{ds} is expected to cause the decrease in the response time; this is actually what we observed.

Effect of the number of V_{gs} pulses on the response time

To explore the synaptic properties of [EMIM][TFSI]-gated P3HT transistors, we applied an increasing number of V_{gs} pulses (5, 10, and 25). As the number of pulses increased, so did the response time. Upon application of a V_{gs} pulse, ions move towards/into the channel materials (Fig. 3). With increasing the number of pulses, the time needed for the anions to redistribute in the p-type P3HT increases, since they penetrate deeper into the film, which can include ion traps. This result can be exploited to drive the device transition from STP to LTP. In other words, the repetition of the stimuli leads to a learning process, in our synaptic IGTs.

We observed that $SNDP_{1-5}$ (where $SNDP_{1-n} = (A_n - A_1)/A_1 \times 100$) is 13%, $SNDP_{1-10}$ is 15%, and $SNDP_{1-25}$ is 17%. These values quantitatively describe the evolution of the SNDP index for our synaptic IGTs.

Impact of the pulse duration time on response time

Increasing the pulse duration time brings about more time for the ions to penetrate the channel. This leads to an increase in the de-doping time and, in turn, an increase in the response time upon removal of the V_{gs} bias. According to Fig. 4a and b, increasing the pre-synaptic spike pulse duration time from 10 ms to 9 s, at V_{gs} = −1 V, induces an increase of the amplitude of the excitatory postsynaptic drain–source current (EPSC), suggesting a more important synaptic weight change. Literature on IL-gated P3HT transistors reports response times depending on the specific device structure and operating conditions.[29,40,41] Frisbie *et al.*, observed a response time of

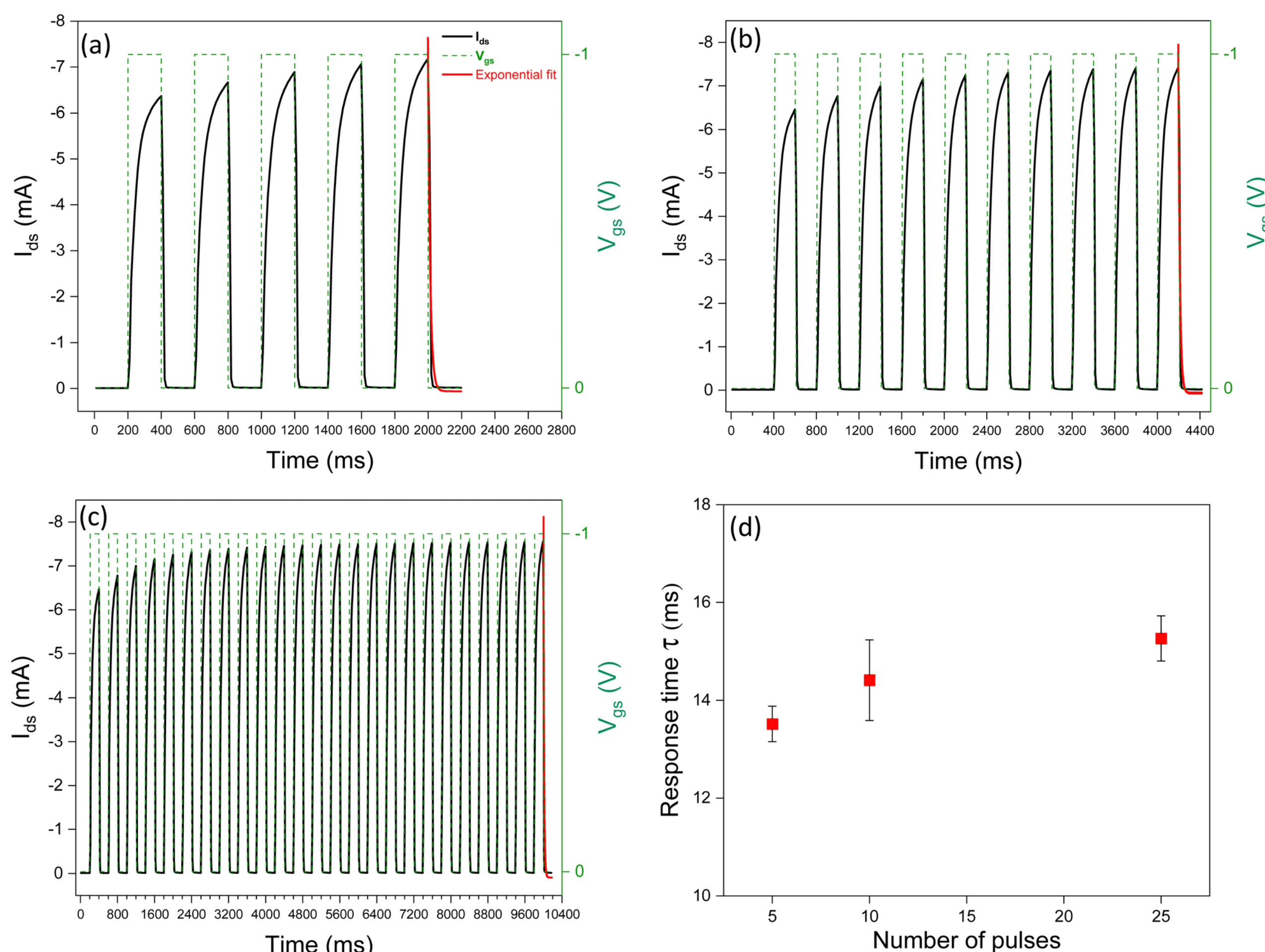

Fig. 3 Transient I_{ds} response of [EMIM][TFSI]-gated P3HT transistors in response to different numbers of V_{gs} square step train pulses. V_{gs} = −1 V at V_{ds} = −0.6 V (a) 5 pulses, (b) 10 pulses, (c) 25 pulses. (d) Response time *versus* number of V_{gs} pulses. The duration and interval of each V_{gs} pulse is 200 ms; exponential fits used to estimate the response time are in red.

 This journal is © The Royal Society of Chemistry 2023

Published on 11 5 2023. Downloaded on 2024-07-16 5:10:48.

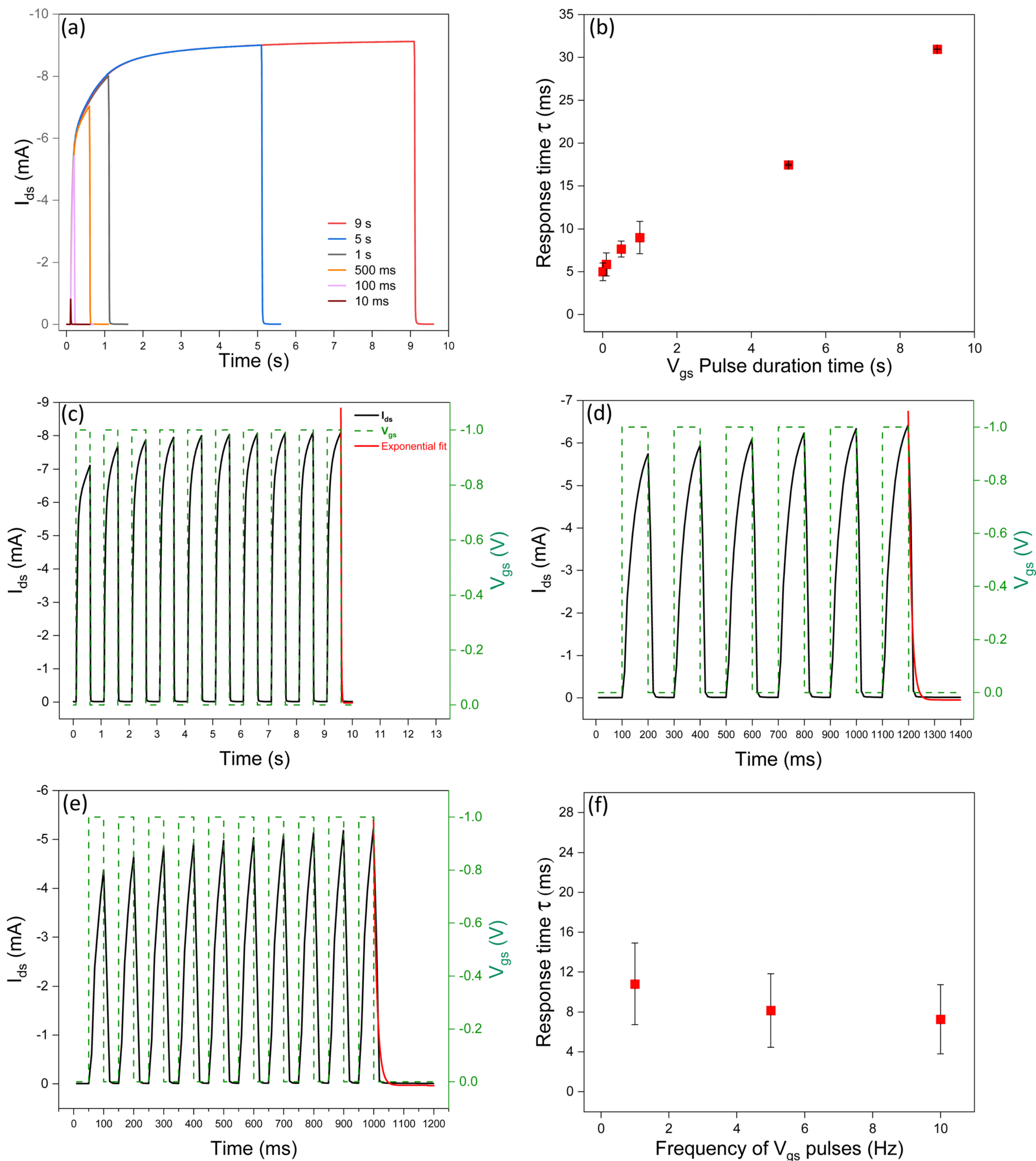

Fig. 4 (a) and (b) Transient I_{ds} characteristic response of an [EMIM][TFSI]-gated P3HT transistor *versus* different duration times. Transient response of transistors in response to V_{gs} pulses with different frequencies (c) 1 Hz, (d) 5 Hz, and (e) 10 Hz. (f) Response time *versus* frequency of V_{gs} pulses (V_{gs} = −1 V, at V_{ds} = −0.6 V).

about 1 ms for ion-gel-gated P3HT transistors with V_{gs} = −3 V and pulse duration of 0.5 ms.[29]

Impact of the frequency of the V_{gs} pulses on the response time

Given the inverse relationship between frequency and pulse duration time, response time is expected to decrease as the frequency of the V_{gs} increases (Fig. 4c–f). This observation is explained by considering that the decrease in the duration time of the V_{gs} pulses brings about a shorter time for ion penetration in the channel (and therefore a shorter depth of penetration of the ions in the P3HT film). This finding is reminiscent of the spike frequency-dependent plasticity (SFDP) of the biological

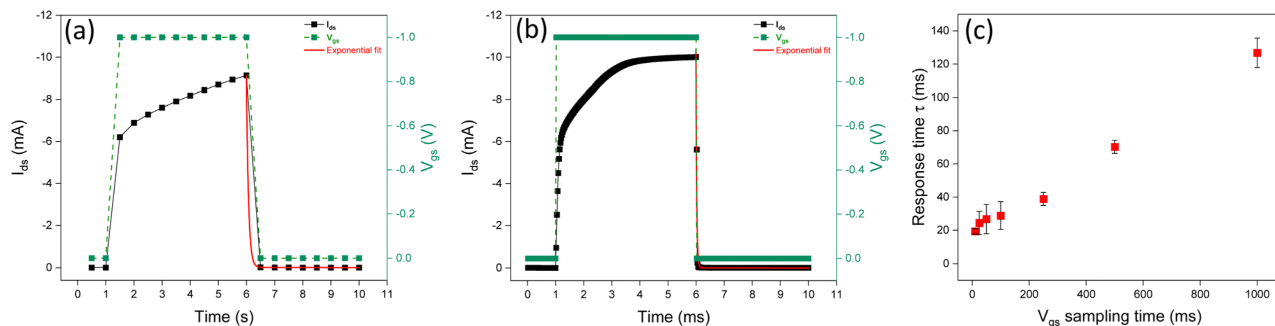

Fig. 5 Transient response of an [EMIM][TFSI]-gated P3HT transistor at different V_{gs} pulse sampling times: (a) 500 ms, (b) 25 ms; the duration of V_{gs} pulse is 5 s. (c) Response time *versus* different V_{gs} sampling times (10, 25, 50, 100, 200, 500, and 1000 ms) at V_{ds} = −0.8 V.

synapses. The SFDP index after six consecutive spikes at frequencies included between 1 Hz and 25 Hz increased from 12% to 15%.

Importance of the V_{gs} sampling time on the measurement of the response time

We investigated the impact of the sampling time of square V_{gs} pulses (with a constant duration time) on the response time. The sampling time is the time difference between two V_{gs} readings taken at two consecutive instants, during the measurement; it permits converting a continuous-time signal into a discrete-time one. By decreasing the sampling time during transient responses, it is possible to obtain more accurate I_{ds} measurements and, in turn, more accurate evaluation of the time response (Fig. 5 and Fig. S3, ESI†).

Experimental

Films of P3HT with regioregular intermediatemolecular weight (50–70 kDa, RIEKE metals), deposited on bare SiO_2/Si substrates, were employed as channel materials of our [EMIM][TFSI]-gated IGTsSiO_2/Si substrates were photolithographically patterned with source and drain electrodes (40 nm-thick Au on a 5 nm-thick Ti adhesion layer) with interelectrode distance, *L*, of 10 μm and width, *W*, of 4 mm. Prior to the deposition of the P3HT films, the substrates were cleaned in sequential steps of 10 min in isopropyl alcohol, 10 min in acetone and 10 min in isopropyl mg P3HT in 1 ml chlorobenzene and stirred overnight in a N_2 glove box (<5 ppm O_2, H_2O).

P3HT films were deposited by spin-coating on the prepatterned SiO_2/Si substrate and placed on a hot plate at 140 °C for 2 hours in the N_2 glove box. [EMIM][TFSI] (IoLiTec, >99%)) was purified under vacuum conditions (*ca* 10^{-5} torr) for 24 hours at 60 °C before use. The ionic liquid was dropped on a DuraporeR membrane (typically 4 mm × 9 mm-sized and 125 μm-thick) located on the transistor channel. The gate electrode was a high surface area of carbon paper (Spectracarb 2050), 6 mm × 3 mm-sized, 170 μm-thick, coated with an ink made of activated carbon (PICACTIF SUPERCAP BP10, Pica, 28 mg ml^{-1}) and polyvinylidene fluoride (PVDF, KYNAR HSV900, 1.4 mg ml^{-1}) binder in *N*-methyl pyrrolidone (NMP, Fluka).

Characterization of the films

Atomic Force Microscopy (AFM) images were taken in the air, at room temperature, on a Digital Instruments Dimension 3100, in tapping mode, with Al-coated silicon cantilevers. X-ray diffraction (XRD) spectra of the P3HT films were taken using a Bruker D8 diffractometer with a wavelength (CuKα) of 1.54 Å. 1100 nm).

Electrical characterization of the devices

Transistor characteristics were obtained using an Agilent B1500A semiconductor parameter analyzer connected to a house-made micromanipulated electrical probe station located in the N_2 glove box.

Conclusions

We studied P3HT-based Ion-Gated Transistors (IGTs) as bio-inspired synapses for applications in neuromorphic systems. We investigated the response time and synaptic plasticity of P3HT IGTs by engineering input stimuli such as values of V_{gs} and V_{ds}, number of pulses of V_{gs}, V_{gs} pulse duration time and frequency.

Response time and plasticity increased with the value of the applied V_{gs} and V_{gs} pulse duration. We were also able to emulate synaptic functions such as short-term plasticity (STP) and long-term plasticity (LTP), and the transition between the two.

We achieved an increased response time *via* repeated V_{gs} presynaptic stimuli (spike number-dependent plasticity (SNDP)) and by decreasing pulse frequency (spike frequency-dependent plasticity (SFDP)), all at low driving voltages (about 1 V).

The relevance of our study is that we demonstrate that IGTs can be employed as neuromorphic devices integrating memory (LTP) and processing functions (STP) in the same device, as a function of the electrical biasing conditions.

Work is in progress to address the effect of the structure of the transistor channel material on the correlation between applied bias conditions and response time, by extending our study to films of P3HT at different molecular weights, other organic semiconductors, and printable metal oxides.

Published on 11 5 2023. Downloaded on 2024-07-16 5:10:48.

This journal is © The Royal Society of Chemistry 2023

View Article Online

Published on 11 5 2023. Downloaded on 2024-07-16 5:10:48.

Author contributions

R. K. A. and C. S. designed the experiments. R. K. A. and T. L. performed the experiments. R. K. A. and C. S. wrote the manuscript. All authors commented on the manuscript.

Conflicts of interest

No conflicts to declare.

Acknowledgements

C. S. acknowledges NSERC (Discovery Grant) for financial support.

References

1 M. Voelker and P. Fromherz, *Small*, 2005, **1**, 206–210.
2 J. J. Jun, N. A. Steinmetz, J. H. Siegle, D. J. Denman, M. Bauza, B. Barbarits, A. K. Lee, C. A. Anastassiou, A. Andrei, Ç. Aydın, M. Barbic, T. J. Blanche, V. Bonin, J. Couto, B. Dutta, S. L. Gratiy, D. A. Gutnisky, M. Häusser, B. Karsh, P. Ledochowitsch, C. M. Lopez, C. Mitelut, S. Musa, M. Okun, M. Pachitariu, J. Putzeys, P. D. Rich, C. Rossant, W. L. Sun, K. Svoboda, M. Carandini, K. D. Harris, C. Koch, J. O'Keefe and T. D. Harris, *Nature*, 2017, **551**, 232–236.
3 C. G. Bischak, L. Q. Flagg, K. Yan, T. Rehman, D. W. Davies, R. J. Quezada, J. W. Onorato, C. K. Luscombe, Y. Diao and C.-Z. Li, *arXiv*, 2019, preprint, arXiv:1910.06440, DOI: 10.48550/arXiv.1910.06440.
4 M. Berggren and A. Richter-Dahlfors, *Adv. Mater.*, 2007, **19**, 3201–3213.
5 J. Rivnay, R. M. Owens and G. G. Malliaras, *Chem. Mater.*, 2014, **26**, 679–685.
6 D. Moia, A. Giovannitti, A. A. Szumska, I. P. Maria, E. Rezasoltani, M. Sachs, M. Schnurr, P. R. Barnes, I. McCulloch and J. Nelson, *Energy Environ. Sci.*, 2019, **12**, 1349–1357.
7 I. E. Jacobs and A. J. Moulé, *Adv. Mater.*, 2017, **29**, 1703063.
8 H. Yuan, H. Shimotani, A. Tsukazaki, A. Ohtomo, M. Kawasaki and Y. Iwasa, *Adv. Funct. Mater.*, 2009, **19**, 1046–1053.
9 L. F. Abbott and S. B. Nelson, *Nat. Neurosci.*, 2000, **3**, 1178–1183.
10 D. A. Bernards and G. G. Malliaras, *Adv. Funct. Mater.*, 2007, **17**, 3538–3544.
11 X. Bu, H. Xu, D. Shang, Y. Li, H. Lv and Q. Liu, *Adv. Intell. Syst.*, 2020, **2**, 2000156.
12 D. Wang, V. Noël and B. Piro, *Electronics*, 2016, **5**, 9.
13 K. Ueno, S. Nakamura, H. Shimotani, A. Ohtomo, N. Kimura, T. Nojima, H. Aoki, Y. Iwasa and M. Kawasaki, *Nat. Mater.*, 2008, **7**, 855–858.
14 J. Rivnay, S. Inal, A. Salleo, R. M. Owens, M. Berggren and G. G. Malliaras, *Nat. Rev. Mater.*, 2018, **3**, 17086.
15 M. J. Panzer and C. D. Frisbie, *Adv. Mater.*, 2008, **20**, 3177–3180.
16 P. Hapiot and C. Lagrost, *Chem. Rev.*, 2008, **108**, 2238–2264.
17 A. Laiho, L. Herlogsson, R. Forchheimer, X. Crispin and M. Berggren, *Proc. Natl. Acad. Sci. U. S. A.*, 2011, **108**, 15069–15073.
18 M. Zakrewsky, K. S. Lovejoy, T. L. Kern, T. E. Miller, V. Le, A. Nagy, A. M. Goumas, R. S. Iyer, R. E. Del Sesto and A. T. Koppisch, *Proc. Natl. Acad. Sci. U. S. A.*, 2014, **111**, 13313–13318.
19 T.-H. Le, Y. Kim and H. Yoon, *Polymers*, 2017, **9**, 150.
20 H. Shimotani, H. Asanuma, J. Takeya and Y. Iwasa, *Appl. Phys. Lett.*, 2006, **89**, 203501.
21 R. Giridharagopal, L. Flagg, J. Harrison, M. Ziffer, J. Onorato, C. Luscombe and D. Ginger, *Nat. Mater.*, 2017, **16**, 737–742.
22 Y. Xia, J. H. Cho, J. Lee, P. P. Ruden and C. D. Frisbie, *Adv. Mater.*, 2009, **21**, 2174–2179.
23 J. O. Guardado and A. Salleo, *Adv. Funct. Mater.*, 2017, **27**, 1701791.
24 E. M. Thomas, M. A. Brady, H. Nakayama, B. C. Popere, R. A. Segalman and M. L. Chabinyc, *Adv. Funct. Mater.*, 2018, **28**, 1803687.
25 V. Kaphle, S. Liu, A. Al-Shadeedi, C. M. Keum and B. Lüssem, *Adv. Mater.*, 2016, **28**, 8766–8770.
26 K. Izutsu, *Electrochemistry in nonaqueous solutions*, John Wiley & Sons, 2009.
27 L. Kergoat, L. Herlogsson, D. Braga, B. Piro, M. C. Pham, X. Crispin, M. Berggren and G. Horowitz, *Adv. Mater.*, 2010, **22**, 2565–2569.
28 M. J. Earle, J. M. Esperança, M. A. Gilea, J. N. Canongia Lopes, L. P. Rebelo, J. W. Magee, K. R. Seddon and J. A. Widegren, *Nature*, 2006, **439**, 831–834.
29 J. H. Cho, J. Lee, Y. He, B. S. Kim, T. P. Lodge and C. D. Frisbie, *Adv. Mater.*, 2008, **20**, 686–690.
30 S. L. Jackman and W. G. Regehr, *Neuron*, 2017, **94**, 447–464.
31 X. Bu, H. Xu, D. Shang, Y. Li, H. Lv and Q. Liu, *Adv. Intell. Syst.*, 2020, **2**, 2000156.
32 L. F. Abbott and W. G. Regehr, *Nature*, 2004, **431**, 796–803.
33 M. A. Lynch, *Physiol. Rev.*, 2004, **84**, 87–136.
34 E. M. Thomas, B. C. Popere, H. Fang, M. L. Chabinyc and R. A. Segalman, *Chem. Mater.*, 2018, **30**, 2965–2972.
35 B. C. Popere, G. E. Sanoja, E. M. Thomas, N. S. Schauser, S. D. Jones, J. M. Bartels, M. E. Helgeson, M. L. Chabinyc and R. A. Segalman, *J. Mater. Chem. C*, 2018, **6**, 8762–8769.
36 L.-a Kong, J. Sun, C. Qian, Y. Fu, J. Wang, J. Yang and Y. Gao, *Org. Electron.*, 2017, **47**, 126–132.
37 C. Qian, L.-a Kong, J. Yang, Y. Gao and J. Sun, *Appl. Phys. Lett.*, 2017, **110**, 083302.
38 P. Gkoupidenis, N. Schaefer, B. Garlan and G. G. Malliaras, *Adv. Mater.*, 2015, **27**, 7176–7180.
39 C. Qian, J. Sun, L. Zhang, H. Huang, J. Yang and Y. Gao, *J. Phys. Chem. C*, 2015, **119**, 14965–14971.
40 D. Rawlings, E. M. Thomas, R. A. Segalman and M. L. Chabinyc, *Chem. Mater.*, 2019, **31**, 8820–8829.
41 G. D. Spyropoulos, J. N. Gelinas and D. Khodagholy, *Sci. Adv.*, 2019, **5**, eaau7378.